Ultramicroscopy 42–44 (1992) 483–489
North-Holland

ultramicroscopy

In situ observation of epitaxial growth of Co thin films on Cu(100)

A.K. Schmid and J. Kirschner
Institut für Experimentalphysik, Freie Universität Berlin, Arnimallee 14, W-1000 Berlin 33, Germany

Received 12 August 1991

The magnetic and electronic properties of ultrathin Co films have been found to depend sensitively on their growth and structure. Therefore, we studied the evolution of Co films during their deposition onto Cu(100) substrates under UHV conditions by STM. Our STM-design offers a simple way to retrieve particular positions on a sample even after preparations like sputtering or annealing, which require multiple sample transfers to a preparation stage. We have observed the nucleation and growth of individual Co islands during the growth of films from the sub-monolayer regime up to several monolayers. At room temperature, the system exhibits epitaxial growth in a nearly ideal layer-by-layer mode. The density of island nucleation is significantly higher in the growth of the first monolayer, compared with additional layers. The onset of growth of the second layer is well before the completion of the first layer, contrasting the more perfect growth of subsequent layers.

1. Introduction

Since early reports [1,2], Co deposited onto Cu(100) under ultrahigh-vacuum (UHV) conditions has quickly evolved into a benchmark system for the research on magnetic ultrathin films. At least up to a film thickness in the range of several tens of monolayers, Co grows pseudomorphically onto the Cu(100) substrate. The film thus assumes a face-centered cubic (fcc) crystal structure, in contrast to the natural room-temperature structure of bulk Co, which is hexagonally close-packed (hcp). This fact had led to the anticipation of interesting electronic and magnetic properties [2]. The system has been studied extensively using various electron scattering techniques LEED, MEED, Auger scattering [1,2], angle-resolved Auger scattering [3], SPSEM [4], photoemission techniques [5], He scattering [1], X-ray scattering [6] and others. The results reported by different groups are, however, sometimes contradictory: for example, a single monolayer of Co on Cu(100) has been found by one group to be ferromagnetic at room temperature [7], whereas other results indicate that the Curie temperature of such a single monolayer film is below 50 K [1]. We believe that some of these differences may be due to differences in the growth conditions. In order to thoroughly study growth behavior, the experimental techniques used previously cannot provide enough detail, as they possess a limited spatial resolution either within the sample surface plane or in the direction normal to it.

The scanning tunneling microscopy (STM) experiment constitutes an ideal complement to those previous investigations. UHV-STM is therefore increasingly being implemented as a new tool to study the growth of metallic ultrathin films [8–11]. The high spatial resolution readily available to this technique, along with the three-dimensional information contained in topographic STM data, enhances the understanding of thin film growth. We have constructed a UHV-STM and investigated the growth of Co on Cu(100).

2. Experiments and methods

A traditional problem of STM is the difficulty of imaging at low magnification, i.e. working with

large image sizes. For this reason, the capability of most STM's to search for a particular location on a sample surface in order to perform a high-magnification study is quite limited. This means, that once a sample is removed from the STM for preparation purposes like sputtering or annealing, a previously imaged region usually cannot be found back for a close study of the effects of the preparation.

The usual approach to solve this problem is based on the idea to expose a sufficiently large sample surface region to a sufficiently homogeneous preparation treatment, so that high-magnification STM images can be taken to be representative of the entire sample surface. The necessity to overcome this problem has long been recognized [12]. For our investigations of thin film growth, we have designed an STM which solves the problem in a different way [13]. The structure of this STM is derived from older, yet very successful designs [14,15]. To the authors' knowledge, however, an important capability of this type of STM has, to this time, not been utilized: particular sample surface regions can be retrieved after transferring samples from the STM and back.

The STM structure is based on an arrangement of mechanical stops, which guide a sample into a fixed position with respect to the STM tip. Although the accuracy of the mechanical stops is crude (repeatability ~ 2–3 μm), the piezo scanner, providing a range of nearly 10 μm, usually allows us to compensate any offsets due to the inaccuracy of the stops. After preparation, samples are transferred into the STM and an image of low magnification is generated. In this image, surface features known from previous work are identified. Then, the scan size is reduced, including appropriate offset, to zoom in on specific regions marked by such features. We wish to point out that this capability is achieved not through complex x–y coarse adjustment arrangements but instead through the sacrifice of such adjustabilities.

To study thin film growth, ideally one would like to have an STM capable of quickly producing images at a high repetition rate *during* the film deposition process. For one main reason, such an ideal experiment is rather difficult to realize. Metal vapor has a very high sticking probability on most surfaces, e.g. on the surface of an STM-tip. Therefore, if the film is deposited while the sample is being imaged by an STM, the tip of the STM would actually shadow the substrate region currently being imaged from the metal vapor. The general approach in the earlier STM metal film studies was thus to deposit a film first and later transfer it into the STM to study it.

To provide the capability of producing STM images with a significantly higher resolution in deposition time, we have chosen to grow films onto the substrate while it is installed in the STM, with the tip approached to within piezo range of the surface, but with the tip lifted off the surface by activation of the z-piezo-element. Our z-piezo can raise the tip several μm; with the metal vapor beam oriented at a conveniently large angle from the surface normal (60°–80°), this arrangement prevents the tip-shadow effect for most of the sample surface. The method allows us to conveniently image a region on the substrate surface, lift the tip off the surface using the z-piezo to deposit a small amount of metal, and after releasing the z-piezo to image again the same location on the sample surface. This sequence can be repeated a large number of times, in order to observe the evolution of a film.

As is well known, the quality of STM images is strongly influenced by the tip morphology [16]. Our method immediately raises legitimate questions about the stability of the morphology of our tip, since, along with the sample, the tip is exposed to the metal vapor beam and thus receives a metal coating. Our experimental results indicate that this is not a problem. In fact, after exposure to the metal vapor, if the tip showed any change in imaging quality at all, the resolution and noise level usually improved rather than deteriorated. As an explanation for this finding, we suggest that the potential increase in tip apex radius due to the deposition of a few monolayers of metal must be negligible. Sometimes, however, image noise can be due to contaminations like oxygen, adsorbed to the tip apex. The material coming from the metal evaporator is highly pure; therefore there is a tendency for potential con-

taminations to be buried and the tip then to become less noisy.

3. Results

Before the production of Co films for STM measurements, samples are cleaned under UHV conditions by multiple Ar-ion sputtering and annealing cycles. Fig. 1 demonstrates the effects of a typical sputter–anneal cycle. After the removal of several monolayers from an annealed Cu(100) crystal, figs. 1a and 1b show a characteristic pattern of craters separated by narrow terraces, with linear dimensions typically in the range of 10 nm. The same location on the sample surface, imaged after an anneal cycle of two hours at 800 K, shows terraces with typical widths in the range of 100 nm, still interrupted by small voids, see figs. 1c and 1d. Annealing the Cu(100) sample at

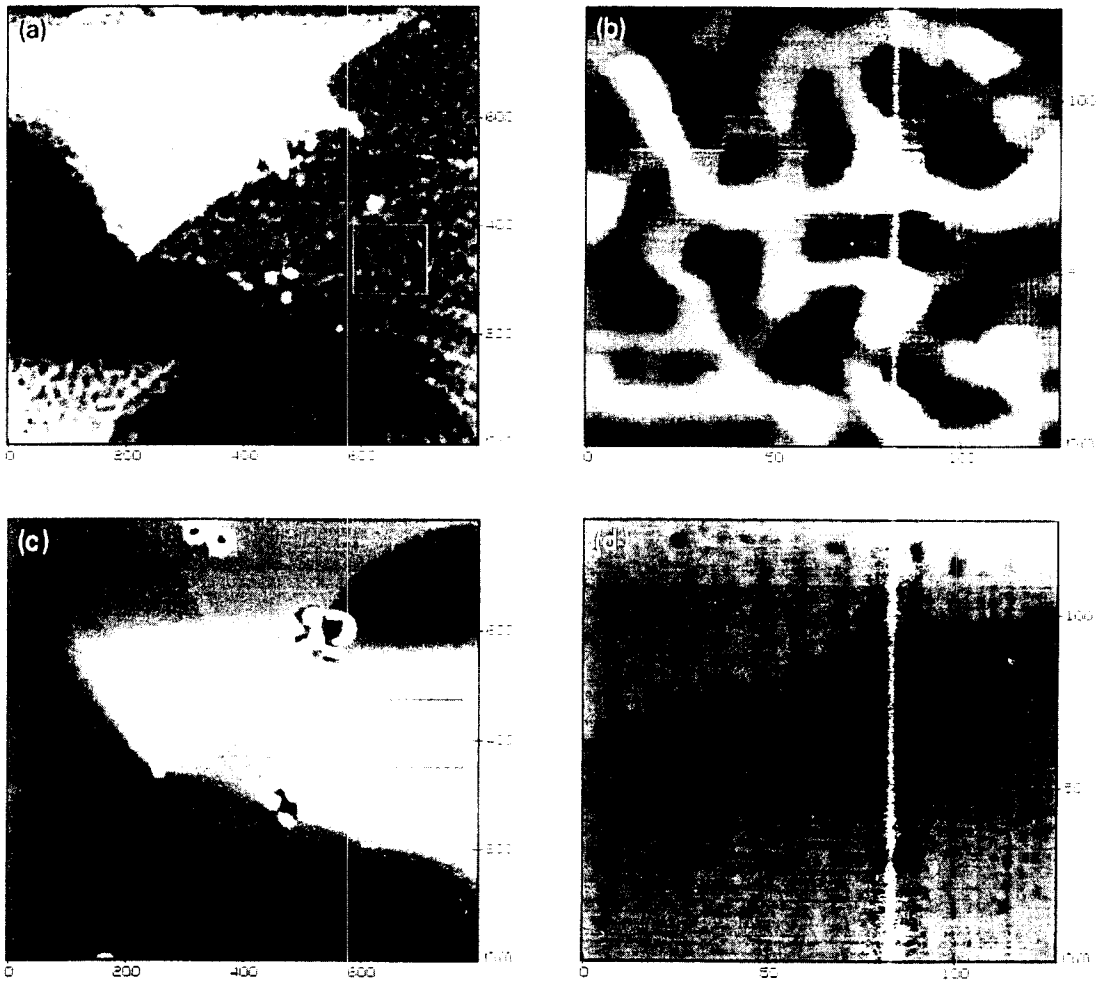

Fig. 1. Local study of the evolution of the surface of a Cu(100) substrate in a typical sputter–anneal cleaning cycle. (a) Shows a pattern of monolayer steps and step-bands, with terraces characteristically disrupted by the ion bombardment. A magnification of a region in (a) (indicated by a box) is shown in (b), typical linear dimensions of the sputtered craters are in the range of 10 nm. The images (c) and (d) show the same location on the surface, smoothed by a soft anneal cycle. Note that for these preparations, the sample had been transferred from the STM stage to a preparation stage and back.

around 900 K for several minutes, atomically flat terraces of several times $\frac{1}{10}$ μm are achieved; with no traces of contaminations detectable by Auger electron spectroscopy.

Onto such surfaces, Co was deposited at rates of around one monolayer per minute, with the sample temperature ranging from 300 to about 330 K. The experiments were performed in UHV with the pressure never exceeding the low 10^{-10} Torr region. Tunneling conditions are usually around 0.5 V positive sample bias and 0.5 nA constant current. We have studied films of up to 6 monolayer thickness. For coverages above two monolayers, the growth was observed to occur in

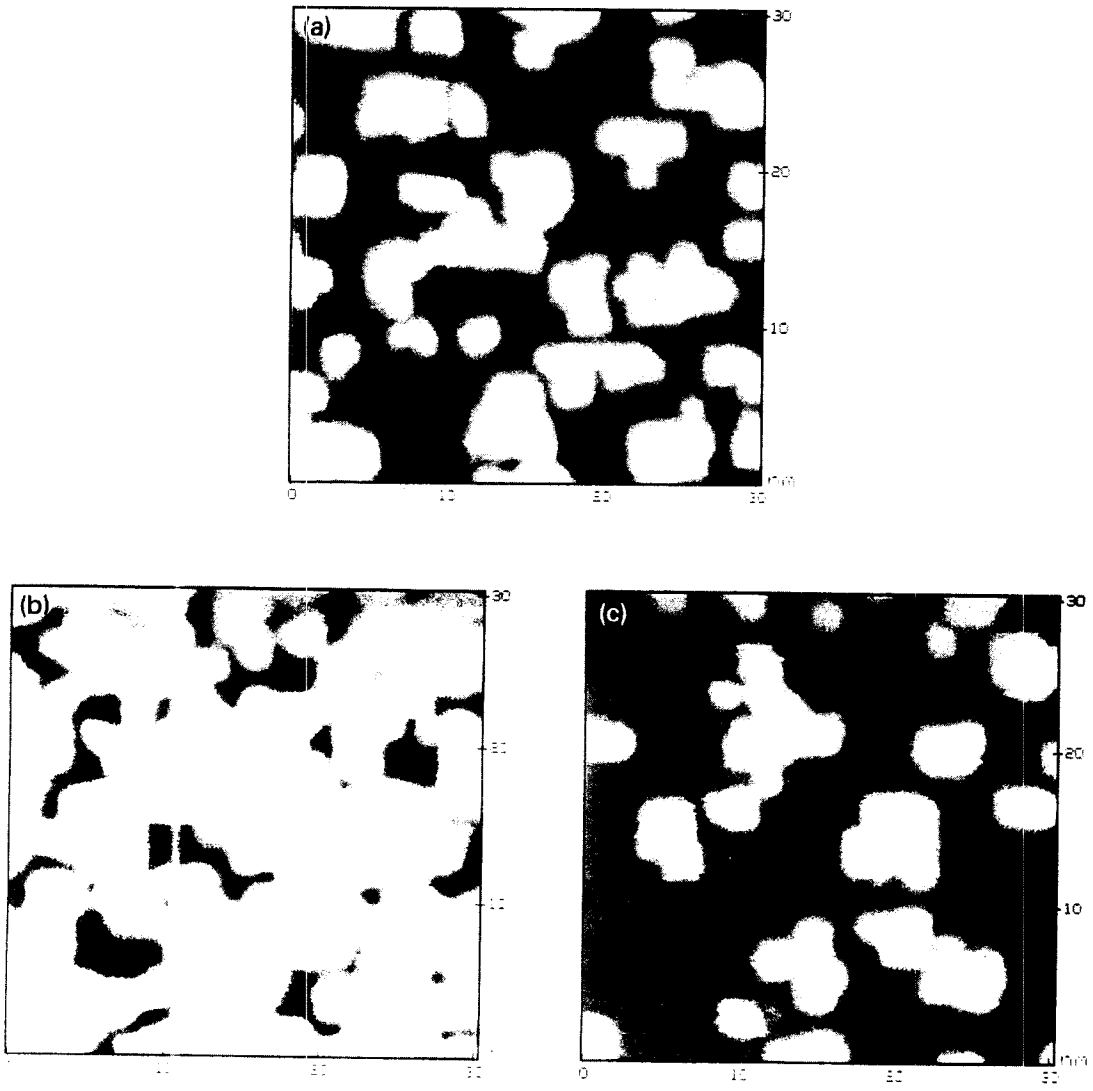

Fig. 2. Typical growth behavior of fcc Co on Cu(100): Co coverages are in (a) 2.5 monolayers, in (b) 2.9 monolayers and in (c) 3.3 monolayers. Surface roughness is decreased in (b), where the third monolayer is nearly completed. Note that white islands in (a) belong to the third monolayer, whereas white islands in (c) belong to the fourth monolayer.

a nearly ideal layer-by-layer mode, see fig. 2. Layers are formed via nucleation of monolayer islands on terraces, as well as at steps.

For half-integral coverages above two monolayers, mean island sizes are typically of the order of 5 to 10 nm linear dimensions. Accordingly, the mean density of monolayer islands at half-integral coverages was found to be $\sim 2 \times 10^4\ \mu m^{-2}$. Usually, the nucleation of islands leading to the formation of an additional monolayer does not occur before the previous layer is nearly completed. Neglecting small deviations, the surface roughness corresponds to ± 1 monolayer at half-integral coverages.

The surface of the films is at no time during the growth found to be as smooth as the underlying Cu(100) substrate. However, with the formation of additional layers, the surface roughness clearly oscillates, being minimal whenever a layer is completed, such as in fig. 2b, where the third monolayer is nearly completed. Aside from these oscillations, surface roughness shows no general increase with growing film thickness in the studied regime of up to 6 layers. The surface roughness of the film seen in fig. 2a, where the third monolayer is nearly half filled, is not significantly different from the surface roughness of the same film after deposition of an additional dose of Co equivalent to an additional monolayer, as shown in fig. 2c.

Concerning the formation of the first two monolayers, the growth mode differs measurably from the generally more perfect layer-by-layer growth mode described above. Recent photoelectron diffraction results [3] have shown that the formation of two-layer thick islands must be significant for average coverages below two monolayers. In this STM study, we find that, first, first-layer islands nucleate in a significantly enhanced density. The island density in a half-filled first layer is $\sim 6 \times 10^4\ \mu m^{-2}$, with island dimensions being accordingly small. Up to a coverage corresponding to around 0.3 monolayers, most islands have a thickness of one monolayer. Upon deposition of additional Co, the growth behavior deviates from the layer-by-layer mode: the first monolayer islands grow in size, and, even though the first monolayer is far from completed, the nucleation and growth of a second monolayer (white areas in fig. 3a) already becomes signifi-

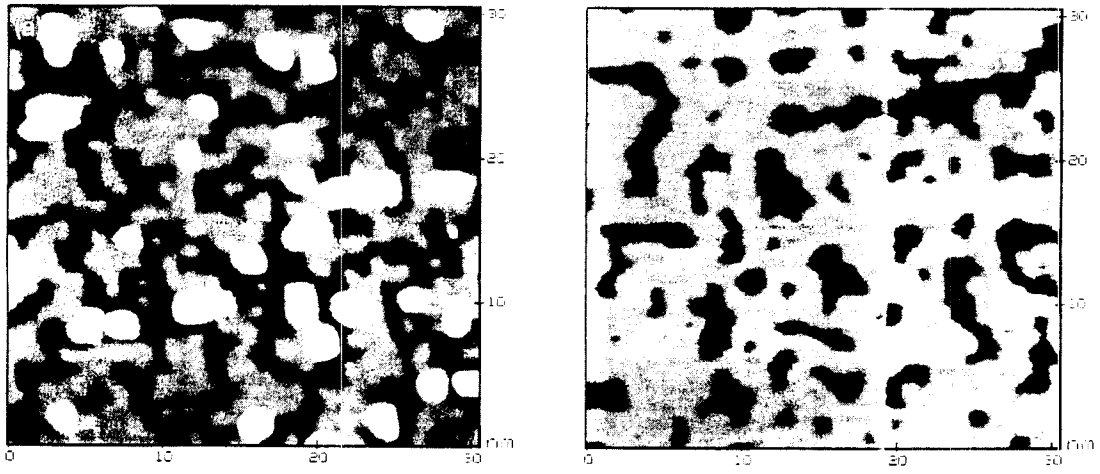

Fig. 3. Typical initial growth behavior of fcc Co on Cu(100). In (a), the areal density of Co is just under one monolayer, in (b) it is just under two monolayers. Characteristically, the first monolayer does not form a closed single sheet: in (a), ~ 30% of the Cu surface (black) is still not covered by the first layer of Co (grey), yet ~ 10% of the second layer (white) has already formed on top of first-layer islands. After deposition of one additional monolayer, the same sample position is shown in (b). The formation of the third layer (here white, one island on the right) does not become significant before the second layer (here grey) is nearly completed.

cant. However, the third monolayer (one white island in fig. 3b) shows no significant nucleation before the underlying bilayer is practically completed: this is the onset of the nearly ideal layer-by-layer growth mode described above.

At all stages during growth, regions showing two types of characteristic deviations from ideal layer-by-layer growth can be found: (1) voids in previous layers, which have not been filled even though the formation of additional monolayers is in full progress, or, (2) monolayer islands which have nucleated and grown prematurely on top of islands belonging to a layer which is still far from completion. The density of these defects is at least one order of magnitude lower than the typical monolayer island density at half-integral coverage. The size of these defects is smaller than typical island sizes found at half-integral coverage. Thus, the combined surface area, of all regions of deviating character amounts to less than 10% of the total surface area of the film; this shall be noted in defense of the term "layer-by-layer growth", used here for a system showing a notable density of defects.

Upon close inspection, both the described types of deviation from ideal layer-by-layer growth can be found, e.g., in fig. 4b. In this image, the Co coverage corresponds to 1.8 monolayers. Most of the surface appears in a light shade of grey, corresponding to the nearly completed second monolayer of the fcc Co film. Regions of the first monolayer of Co, which are not covered by the second layer, appear as a darker shade of grey. A few black voids in the dark grey first layer are apparent (deviations of type (1)). Also, a few white islands, belonging to the third monolayer of Co (deviations of type (2)), can be found on top of the light grey second layer.

The shapes of Co monolayer islands or voids tend to reflect the symmetry of the substrate crystal: in the images shown in this paper, (110) directions are horizontal and vertical in the image plain; monolayer edges often follow these directions. The tendency of the crystal symmetry being

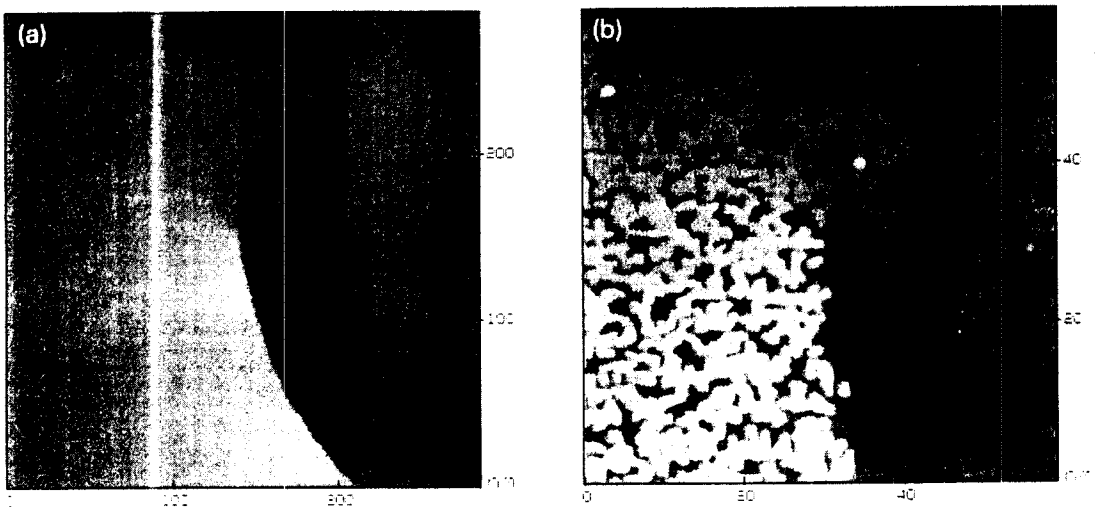

Fig. 4. A $\frac{1}{4}$ μm scan of clean Cu(100) is shown in (a), with one screw dislocation and the monolayer step originating from it being the only defects present. After the deposition of 1.8 monolayers of Co, the same screw dislocation was imaged again (b). (Note the higher magnification in (b).) The dark shade of grey corresponds to the first monolayer, the light shade of grey corresponds to the second monolayer of fcc Co. The Co film has reproduced the monolayer step. No influence of the screw dislocation on the film growth is apparent. A tendency of Co-island edges to follow (110) directions (vertical and horizontal) is apparent. A few small islands of the third monolayer (white), as well as a few small voids in the first layer (black) constitute deviations from ideal layer-by-layer growth.

reflected in the shape of islands and voids can be attributed to the enhanced stability of monolayer steps following (110) directions: this step direction provides the highest coordination number.

Screw dislocations can be found occasionally on the Cu(100) substrate. Although these defects are associated with a long-range stress field, their influence on the growth of fcc Co films seems to be negligible, as seen in fig. 4. Monolayer steps, on the other hand, act as traps for Co. The dominance of island nucleation and growth on terraces causes steps to be reproduced during film growth in nearly their original positions. The monolayer step originating from the screw dislocation in fig. 4 shows up again, in nearly the same place, upon completion of each layer of Co.

4. Conclusions

When deposited onto Cu(100) at room temperature, fcc Co grows in a nearly ideal layer-by-layer mode. The growth process involves nucleation and growth of monolayer islands. Surface roughness oscillates with the formation of monolayers. Deviations from ideal layer-by-layer growth, in particular in the regime of coverages under two monolayers, are observed. An apparent high nucleation density in the deposition of the first monolayer is indicative of a reduced mobility of Co adatoms on Cu, compared with the mobility of Co adatoms on a fcc Co film. In contrast to the nearly ideal two-dimensional growth starting with the buildup of the third layer, second-layer islands nucleate well before the first layer is completed. Characteristically, island shapes reflect the substrate crystal symmetry, with island edges following (110) directions.

The feasibility and value of a STM capable of retrieving particular locations on a sample surface was demonstrated.

Acknowledgement

This work was supported by the Deutsche Forschungsgemeinschaft through Sonderforschungsbereich 6.

References

[1] J.J. De Miguel, A. Cebollada, J.M. Gallego, S. Ferrer, R. Miranda, C.M. Schneider, P. Bressler, J. Garbe, K. Bethke and J. Kirschner, Surf. Sci. 211/212 (1989) 732; C.M. Schneider, P. Bressler, P. Schuster, J. Kirschner, J.J. de Miguel and R. Miranda, Phys. Rev. Lett. 64 (1990) 1059.
[2] L. Gonzales, R. Miranda, M. Salmeron, J.A. Verges and F. Yndurain, Phys. Rev. B 24 (1981) 3245.
[3] H. Li and B.P. Tonner, Surf. Sci. 237 (1990) 141.
[4] H.P. Oepen, M. Bennig, H. Ibach, C.M. Schneider and J. Kirschner, J. Magn. Magn. Mater. 86 (1990) L137.
[5] J.J. de Miguel, A. Cebollada, J.M. Gallego, R. Miranda, C.M. Schneider, P. Schuster and J. Kirschner, J. Magn. Magn. Mater. 93 (1991) 1.
[6] S. Ferrer, E. Vlieg and I.K. Robinson, Surf. Sci. Lett. 250 (1991) L636.
[7] D. Pescia, G. Zampieri, M. Stampioni, G.L. Bona, R.F. Willis and F. Meier, Phys. Rev. Lett. 58 (1987) 933; T. Beier, H. Jahrreiss, D. Pescia, Th. Woike and W. Gudat, Phys. Rev. Lett. 61 (1988) 1875.
[8] J. Wintterlin and R.J. Behm, in; Scanning Tunneling Microscopy I, Eds. R. Wiesendanger and H.J. Güntherodt (Springer, Berlin, in press).
[9] D.D. Chambliss and R.J. Wilson, J. Vac. Sci. Technol. B 9 (1991) 928.
[10] D.D. Chambliss and S. Chiang, J. Vac. Sci. Technol. B 9 (1991) 933.
[11] A. Brodde, G. Wilhelmi, D. Badt, H. Wengelnik and H. Neddermeyer, J. Vac. Sci. Technol. B 9 (1991) 920.
[12] R. Möller, A. Esslinger and M. Rauscher, J. Vac. Sci. Technol. A 8 (1989) 434.
[13] A.K. Schmid and J. Kirschner, J. Vac. Sci. Technol. B 9 (1991) 648.
[14] W.J. Kaiser and R.C. Jaklevic, Surf. Sci. 181 (1987) 55.
[15] B. Drake, R. Sonnenfeld, J. Schneir and P.K. Hansma, Surf. Sci. 181 (1987) 92.
[16] Y. Kuk and P.J. Silvermann, Appl. Phys. Lett. 48 (1986) 1597.